SYNTHESIS OF Na-A ZEOLITE FROM 10 Å HALLOYSITE AND A NEW CRYSTALLIZATION KINETIC MODEL FOR THE TRANSFORMATION OF Na-A INTO HS ZEOLITE

DANIELA NOVEMBRE[1], BRUNO DI SABATINO[1] AND DOMINGO GIMENO[2],*

[1] Dipartimento di Scienze della Terra, Università degli Studi 'G.D'Annunzio' Via dei Vestini 30, 66013 Chieti, Italy
[2] Departamento de Geoquímica, Petrología y Prospecció Geològica, Universitat de Barcelona, 08028 Barcelona, Spain

Abstract—The present work deals with the synthesis of Na-A zeolite using 10 Å halloysite (collected near Grosseto, Italy) as the starting material, instead of the more expensive chemicals currently used in industry (Na aluminates and Na silicates). The process of synthesizing Na-A zeolite from 10 Å halloysite is rather simple as the reaction of halloysite with alkali occurs very readily and is achieved without prior thermal activation at high temperature. The optimal conditions of crystallization of Na-A zeolite from 10 Å halloysite are reached at 80°C. At lower temperatures, transformation of halloysite into an amorphous material requires more time, and the field within which Na-A zeolite exists overlaps that of 7 Å halloysite, G and HS zeolites. The products of synthesis at 80°C were characterized by X-ray diffraction, scanning electron microscopy, inductively coupled plasma optical emission spectrometry and infrared spectroscopy. We also propose a model to study the reaction kinetics of zeolite (Na-A and HS) nucleation and growth by real-time X-ray powder diffraction data.

Key Words—10 Å Halloysite to 7 Å Halloysite Transformation, Na-A Zeolite Synthesis, Natural Halloysite.

INTRODUCTION

Zeolite synthesis from clay minerals has been investigated to a great extent in recent decades due to the large availability of raw clay materials, their relatively low cost and their adequate chemical characteristics (*e.g.* Aznar and La Iglesia, 1985; Clifton, 1987; Akokelar *et al.*, 1997; Gualtieri *et al.*, 1997). Previous studies focused in particular on the use of kaolinite, because of its extensive availability and the well known reactivity of thermally treated kaolin clays (metakaolin) with alkali solutions (*e.g.* Madani *et al.*, 1990; Rocha and Klinowski, 1991; Gualtieri *et al.*, 1997; Akokelar *et al.*, 1997; Demortier *et al.*, 1999).

Numerous researchers have also explored the utility of halloysite as the zeolite precursor taking into account the chemical and structural similarities between halloysite and kaolinite (Aznar and La Iglesia, 1985; Gualtieri, 2001).

Franco and Aiello (1968) studied the direct hydrothermal zeolitization of halloysitic tuffs under hydrothermal alkaline conditions in the temperature range 200–300°C, producing analcime and phillipsite. Takahashi and Nishimura (1968) treated halloysite of very low crystallinity with commercial glass (to increase the Si/Al ratio) under hydrothermal alkaline (NaOH) conditions. This resulted, at 50°C, in destruction of the halloysite structure, then at 70°C initial crystallization of

faujasite, and finally, at 90°C rapid formation of faujasite followed by a decrease of this phase by transformation into hydroxysodalite. The same authors (1967) also reported the formation of zeolite A from halloysite under ambient conditions.

Aiello and Franco (1968) processed halloysite and montmorillonite under alkaline hydrothermal conditions (80°C) obtaining A, Na-P, K-F, HS and chabazite zeolites. La Iglesia *et al.* (1974) produced zeolite A and faujasite at 35°C under alkaline conditions starting from a natural halloysite activated by dry grinding for 5 h.

Aznar and La Iglesia (1985) developed a set of experiments using several types of clays (but not halloysite) under hydrothermal alkaline conditions (60, 70 and 90°C). These clays were used in their native form in experiments, and also after pre-treatment (dehydroxylation). They concluded that the best results for synthesis of zeolites A and X are obtained from thermally activated kaolinitic clays. They provided evidence that high hydrothermal temperatures favor high crystallization velocities, low temperatures favor growth of zeolite X over zeolite A, and addition of crystal seeds decreases the total reaction time by eliminating the nucleation step. In the experiments with clays which have not been dehydroxylated, these authors only reached synthesis of HS zeolite and phillipsite.

Gualtieri (2001) obtained Na-X, Na-P and analcime from halloysite from natural hydrothermalized leucitic tuffites (this material also contained 50 wt.% of finely interdispersed amorphous silica). This research explored the similar behavior of kaolin and halloysite. It followed

28

the same path of kaolin-based experiences: thermal activation of halloysite at 600ºC prior to soaking it in NaOH solution in the temperature range 90−150ºC.

One can conclude from these studies that the formation of metastable zeolites A and X is greatly enhanced under low-temperature and low-autogen pressure using Na solutions and thermally activated Al clays.

Na-A zeolite is largely used by the detergent industry in countries with restrictive environmental regulations (Chiaudiani *et al.*, 1988). The synthetic zeolite substitutes Na tripoliphospate (NTP) which is considered one of the main pollutants responsible for the eutrophization of superficial waters, particularly in North America (large lakes) and the Alpine-Adriatic sea area in Europe (Chapra, 1977; Chiaudiani *et al.*, 1988; Cardoso *et al.*, 2001). Industries currently synthesize Na-A zeolite from pure chemical products: NaOH solutions, Na silicates, pure $Al(OH)_3$ and Na aluminates. In order to reduce the synthesis costs, research is turning to the use of alternative and less expensive natural materials. From an economic point of view, the use of halloysite has great potential because large volumes of inexpensive pyroclastic volcanic rocks contain halloysite as a common secondary mineral formed by alteration of alkaline volcanic glasses.

The aim of the present work is to synthesize pure Na-A zeolite at low temperature using a pure natural halloysite without prior thermal activation at high temperatures; this would represent a considerable economic advantage in terms of energy consumption and cost of raw materials. Also, we propose a mathematical model of the crystallization kinetics for a macroscopic two-component system applicable to zeolites formed by thermal treatment of 10 Å halloysite with NaOH solutions.

MATERIALS

Halloysite from Capalbio (near Grosseto, Italy) was used as the starting material. The Capalbio deposit was mined for Fe and Mn sulfides in the past. Halloysite was interpreted as a direct precipitate from acid solutions filling vugs, lenses and geodic cavities inside deeply hydrothermally altered metamorphic rocks (Di Sabatino *et al.*, 1996). This halloysite shows great purity (Table 1). This is remarkable because of its low Fe content (0.21 wt.%, Table 1) as well as the absence of rutile and scarcity of zircon accessory phases. A chemical analysis of a white halloysite by Kerr *et al.* (1950) is reported in Table 1 for comparison.

The structure of 7 Å and 10 Å halloysite is disordered. The open structure of 10 Å halloysite allows intercalation of H_2O molecules. Its ideal chemical formula is $Al_2Si_2O_5(OH)_4 \cdot nH_2O$.

The intercalated water is lost at 180ºC, resulting in the collapse of halloysite layers down to 7 Å. Comparison of halloysite with Na-A zeolite

$(6(NaAlSiO_4 \cdot 2.2H_2O))$ indicates the chemical similarity of the two minerals. Additions of NaOH solutions to 10 Å halloysite should actually lead to a perfectly stoichiometric Na-A zeolite. We note also that the structure of 10 Å halloysite is basically the same as that of kaolinite (Si tetrahedral sheets joined to Al octahedral sheets by sharing a plane of oxygens, *e.g.* Costanzo and Giese, 1985), with kaolinite being the most common phyllosilicate involved in successful zeolite A synthesis (*e.g.* Aznar and La Iglesia, 1985; Madani *et al.*, 1990; Rocha and Klinowski, 1991; Gualtieri *et al.*, 1997; Akokelar *et al.*, 1997; Demortier *et al.*, 1999).

METHODS

The starting material (10 Å halloysite) was characterized by XRD analysis (Figure 1), using a Philips diffractometer PW 1710 (CuKα = 1.518, 40 kV, 20 mA, 3−40º2θ range, 0.020º2θ per step, 5 s per step).

The most favorable conditions for the synthesis of zeolite A were selected, taking into account the results of earlier experiments, to minimize both energy and reaction time. Several hydrothermal experiments were conducted at room pressure and various low temperatures (45, 65 and 80ºC).

Periodically collected samples were analyzed by XRD to identify each step of the halloysite transformation and Na-A synthesis. Samples collected at different time intervals were washed thoroughly with distilled water and oven dried at 40ºC for 24 h. The powder samples were prepared as smears on glass slides; the mineral composition of each sample was determined using the XRD peak positions and intensities (XRD JCPDS codes).

Infrared (IR) spectroscopy was used to characterize the transformation of gel into Na-A zeolite and then into HS (hydroxysodalite) in the experiment performed at

Table 1. Chemical composition of starting material HAL-CAP (after Di Sabatino *et al.*, 1996) and of halloysite HALL-WH (after Kerr *et al.*, 1950).

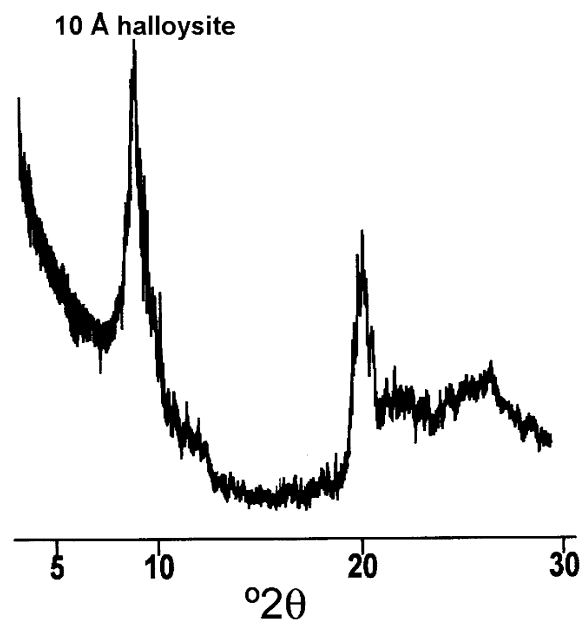|	HAL-CAP	HALL-WH
SiO_2	42.21	44.46
TiO_2	0.01	0.15
Al_2O_3	33.22	36.58
Fe_2O_3	0.21	0.36
FeO	tr.	0.07
CaO	0.12	0.19
MnO	tr.	tr.
MgO	tr.	0.18
Na_2O	tr.	0.01
K_2O	0.01	0.51
P_2O_5	tr.	0.18
H_2O^-	4.8	4.05
H_2O^+	19.62	13.38
Total	100.20	100.12

tr.: trace

10 Å halloysite

Figure 1. XRD pattern of the starting material, Capalbio 10 Å halloysite.

80°C. The IR studies were conducted using a Nicolet 760 spectrometer, served by a beam splitter of KBr and a DTGS detector; the IR radiation source was a SiC (Globar) filament. Samples were prepared following the method of Robert *et al.* (1989a) by means of powder pressed pellets (KBr/sample ratio of 1/100, 10 t/cm^2); spectra were processed using the OMNIC 3.1° program.

Chemical analyses of synthesized zeolites were performed by inductively coupled plasma-atomic emission spectrometry (ICP-AES), through previous alkaline fusion of samples within Pt melt pots (lithium meta-tetra borate pearls, at 3/2 ratio) and subsequent acid solubilization. Each sample was fused in duplicate and melt pots were cleaned each time by alkaline fusion plus acid bath. Standard solutions were prepared each time. The standards were prepared by traditional wet methods from a certified commercial traceable list. International rock standards (provided by the Geological Survey of Japan, GSJ) have been analyzed and used as internal standards.

Morphological observations on the Na-A crystals synthesized at 80°C were on a JEOL J3M-840 SEM served by a LINK Microanalysis EDS system. Operating

conditions were of 10 kV with window conditions ranging from 18 to 22 mm.

Transformation of 10 Å halloysite to Na-A zeolite

Transformation of halloysite in Na-A zeolite was obtained using the following method: the powdery halloysite was placed in a teflon reactor with an alkaline solution (NaOH, 2.5 M) and was held at temperatures of 45, 65 and 80°C, and corresponding water pressure, until transformation into the expected zeolitic phases was completed.

RESULTS AND DISCUSSION

Synthesis at 45°C

10 Å halloysite is not stable in the presence of NaOH at 45°C. Transformation of 10 Å halloysite into 7 Å halloysite occurs within the first 2 h of the alkaline treatment at 45°C (Figure 2). Then, after 8 h, there is a decrease in the intensity of the 7 Å peak, suggesting dissolution or amorphization, allowing nucleation of zeolites. After 10 h, G zeolite appears and, as 7 Å halloysite continues to disappear slowly, G, G+Na-A, and finally G+Na-A+HS zeolites progressively replace halloysite. The experiment fails to produce Na-A zeolite as an isolated zeolitic phase regardless of the run time.

Synthesis at 65°C

Transformation of 10 Å halloysite into 7 Å halloysite at 65°C, in the presence of alkaline solution, occurs more rapidly (<1 h) than for the experiment conducted at 45°C. This results in an increase in chemical reactivity with the bath of alkaline solution (Figure 3). However, 100% crystallization of isolated pure Na-A zeolite is not reached; 7 Å halloysite persistence lengthens the transformation times. Finally, this results in an overlapping of Na-A zeolite with Na-G and HS zeolites.

Synthesis at 80°C

In Figure 4 we report the XRD pattern of the experimental run conducted at 80°C.

Complete consumption of 7 Å halloysite occurs more rapidly (1.5 h) at 80°C (Figure 4) than at 65°C, and G zeolite is not formed. Crystallization of Na-A zeolite begins after only 1.3 h, while the crystallization maximum is reached at 1.45 h. However, the complete

Table 2. IR data for Na-A and HS zeolites synthesized at 80°C.

	Asymmetric stretch	Symmetric stretch	Double rings	T—O bends
Na-A (A$_2$)	1086(MW)-1051(W)-1009(S)	671(MW)	560(MS)	471(M)
Na-A*	1090(MW)-1050(W)-995(S)	660(MW)	550(MS)	464(M)
Na-A**	1100(MW)-1050(W)-1000(S)	665(MW)	555(MS)	465(M)
Na-A***	1000(S)	data not available	550(MS)	data not available
HS (A$_5$)	1090(MW)-986(S)	735(M)-707(MW)-667(M)	/	466(MS)-437(MS)
HS*	1096(MW)-986(S)	729(M)-701(MW)-660(M)	/	461(MS)-432(MS)

* Flaningen *et al.* (1971); ** Rocha and Klinowski (1991); *** Demortier *et al.* (1999)
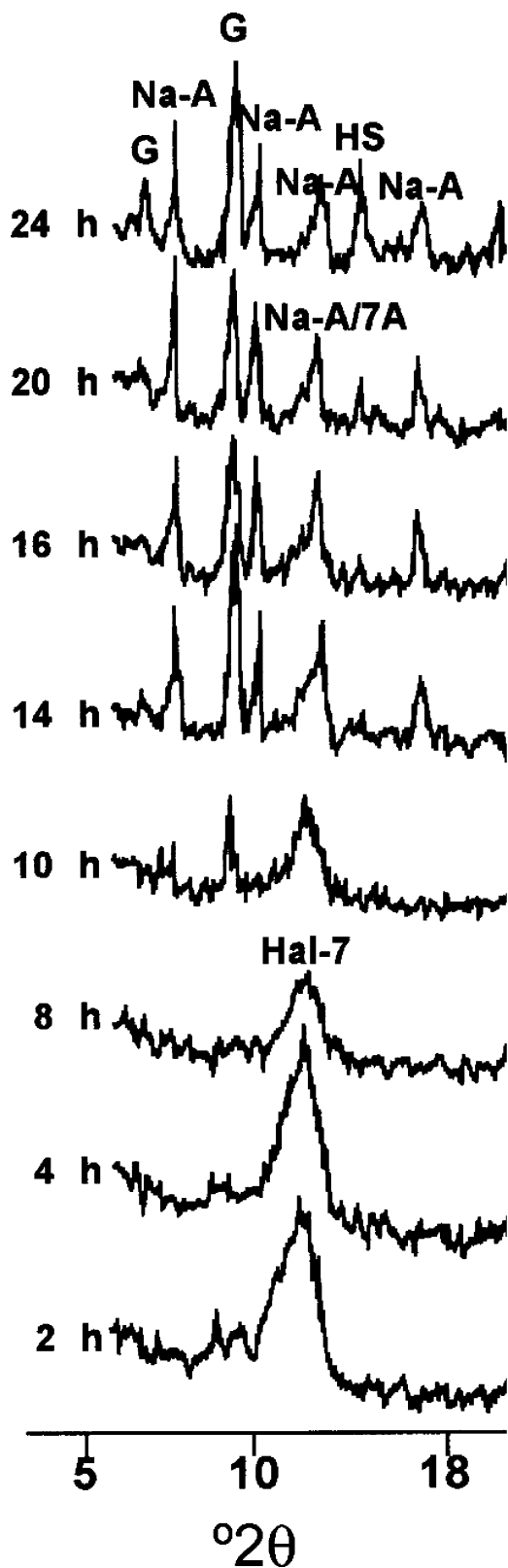
disappearance of halloysite, the field of total crystallization of Na-A zeolite and the beginning of hydroxy-sodalite crystallization still occur after a short period of time.

Fourier transform infrared (FTIR) spectra of the product obtained at 80°C are shown in Figure 5, while band positions for the Na-A and HS phases obtained are reported in Table 2, together with data from Rocha and Klinowski (1991), Demortier *et al.* (1999) and Flaningen *et al.* (1971). Sample A_1 (run duration of 1.15 h) shows the presence of bands at 999, 855, 717 and 594 cm^{-1}. The band at 855cm^{-1} can be assigned to Si-OH

Figure 2. XRD patterns of the synthesis products obtained at 45°C for different run times.
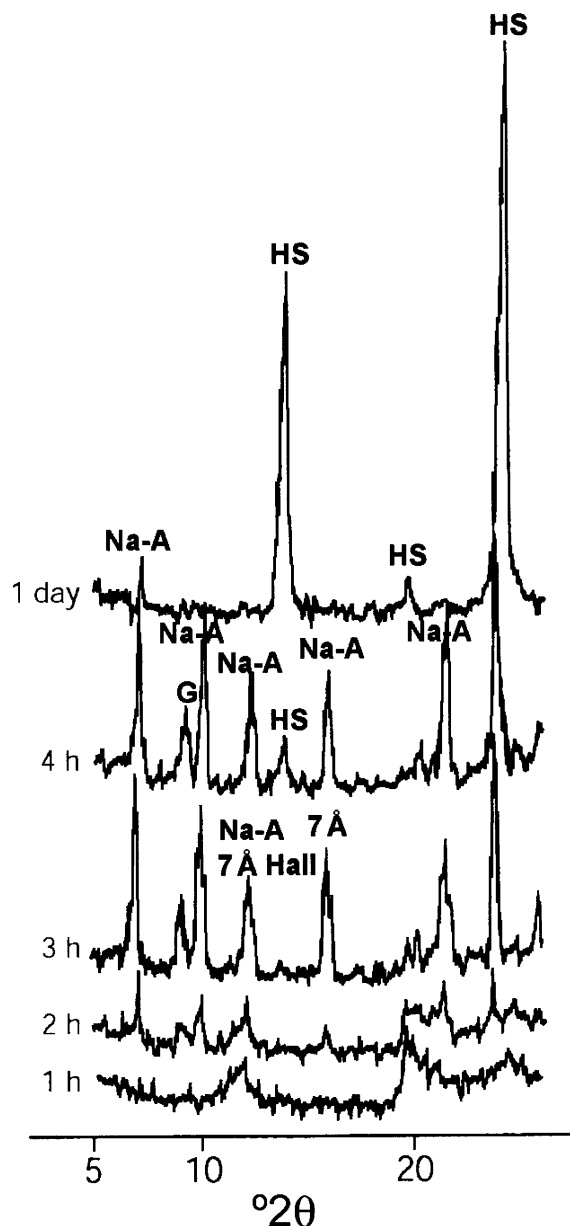

Figure 3. XRD patterns of synthesis products obtained at 65°C for different run times.
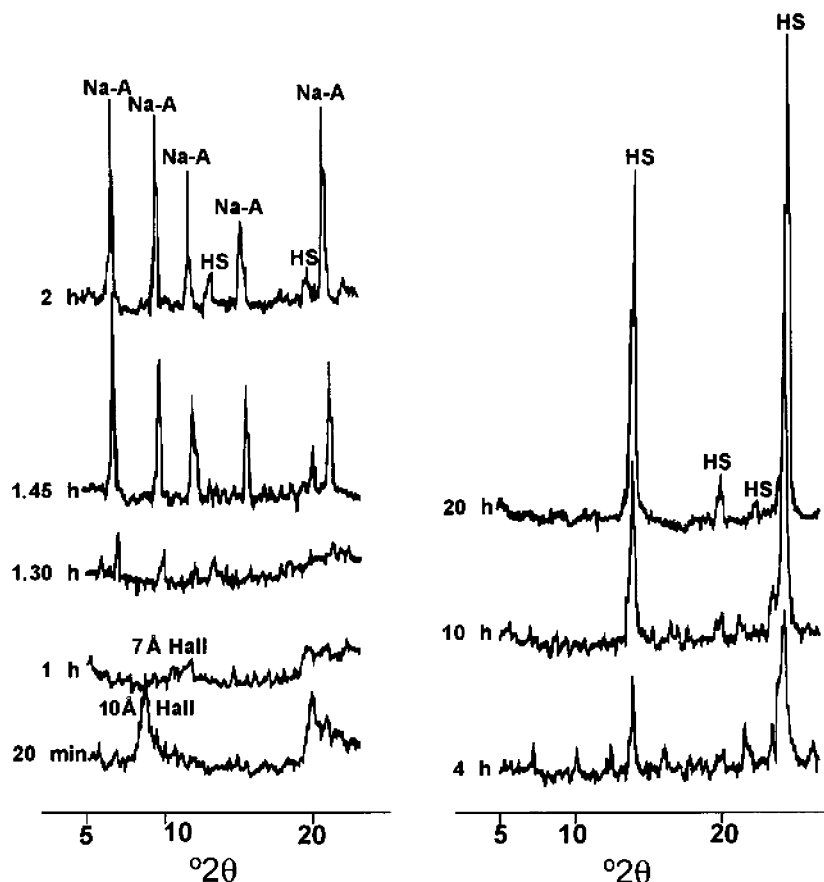
Figure 4. XRD pattern of synthesis products obtained at 80°C for different run times.

stretching; its intensity decreases with increasing crystallinity (as shown by Rocha and Klinowski, 1991); in fact, it disappears at 1.45 h (A_2), the time at which zeolitic crystallization becomes evident, *i.e.* new bands characteristic of Na-A zeolite (Flaningen *et al.*, 1971) at 1086, 1051, 671, 560 and 471 cm^{-1}.

Results of the analyses of the FTIR spectra are in agreement with the evaluations made by Demortier *et al.* (1999) about synthesis of Na-A zeolite from pre-activated metakaolinite. According to those authors, the synthesis of Na-A zeolite from metakaolinite occurs *via* a chemical compound (referred to as a "precursor"), that can be considered an intermediate phase between kaolinite and Na-A zeolite. The 'precursor' is formed during the induction period (Madani *et al.*, 1999) and it is characterized by an XRD pattern consisting of a broad band typical of an amorphous compound, and by an IR spectrum displaying bands different from both those of kaolinite and Na-A zeolite. From these observations sample A_1 can be considered a 'precursor phase' of Na-A zeolite, intermediate between 7 Å halloysite and Na-A zeolite.

Demortier *et al.* (1999) reported a Si/Al ratio of 1.00±0.05 and a Na/Al mole ratio equal to 1 for the 'precursor' as for Na-A zeolite and sodalite. Therefore, from a chemical point of view, the 'precursor' is characterized by the same composition as Na-A zeolite.

Chemical analyses of samples of the run conducted at 80°C are reported in Table 3. Sample A_1 shows a Si/Al ratio of 1.03 and a Na/Al ratio of 0.88; these values are comparable with those of sample A_2 (Na-A zeolite) and with those calculated for a commercial Na-A zeolite (Na-A 4A-UOP), as is shown in Table 3.

Table 3. Chemical analyses of the zeolites synthesized at 80°C.

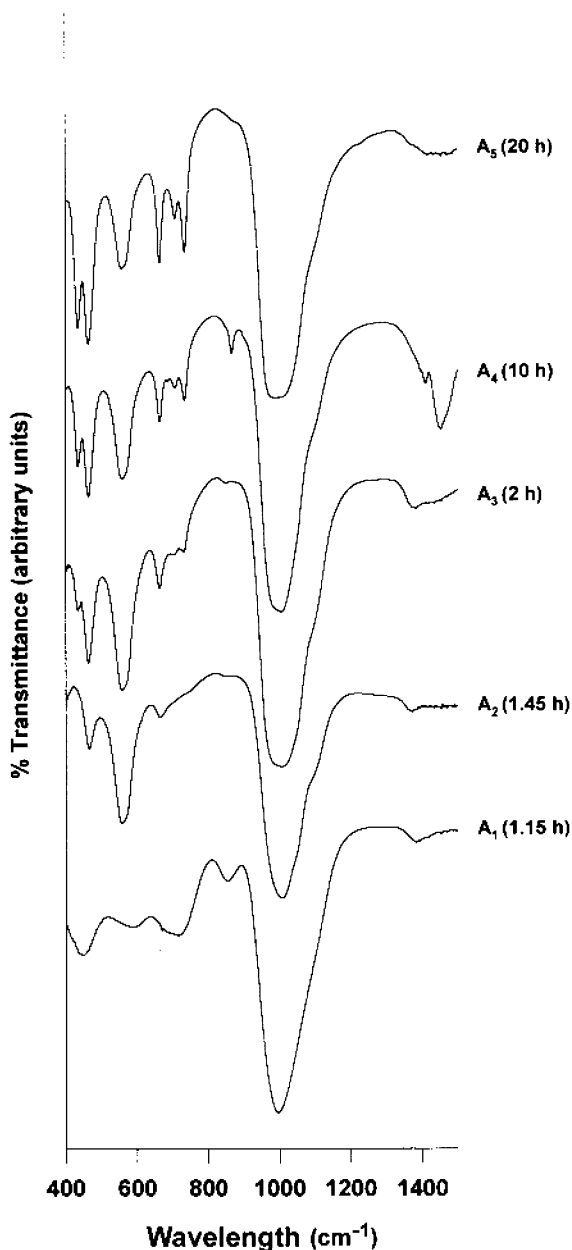| Sample	Na(%)	Si(%)	Al(%)	Na/Al	Si/Al	(Si/Si+Al)	Time (h)	XRD spectrum
A1	12.94	15.12	14.64	0.88	1.03	0.51	1.15	amorphous
A2	12.5	13.35	13.65	0.92	0.98	0.49	1.45	Na-A (S)
A5	16.24	15.75	14.47	1.12	1.09	0.52	20	HS (S)
Na-A 4A-UOP	13.12	13.24	13.77	0.95	0.96	0.49	/	Na-A

Figure 5. IR spectra of the synthesis products obtained at 80°C for different run times.

We can argue, according to Rocha and Klinowski (1991), that once formed, the 'precursor' is transformed into Na-A zeolite by a structural rearrangement without further changes in composition.

A MATHEMATICAL MODEL FOR CRYSTALLIZATION KINETICS

We created a mathematical model of crystallization kinetics for a macroscopic two-component system. We then applied the mathematical model to fit data for the experimental run carried out at 80°C, related to crystal-lization of Na-A zeolite that is later replaced by HS zeolite.

For this kind of phenomenon, the approach suggested by Avrami (1939), related to the nucleation and growth in the crystallization kinetics process, can be expressed as:

$$X = 1 \; e^{(-K_A t^n)} \tag{1}$$

where X is the actual fraction of the material transformed, n is the Avrami index and K_A is an overall rate constant of crystallization (Van Krevelen, 1978). Next, the crystallization half-time ($X = 50\%$) can be calculated from equation 1 as:

$$t_{1/2} = \left(\frac{\ln 2}{K_A} \right)^{1/n}$$

the factor K_A depends on both the rate of diffusive transport of the molecules in the solution and the free energy of a crystal nucleus growing in the space (Van Krevelen, 1978; Ehrun, 1992). By considering only the first-order Taylor approximation of equation 1 we obtain the following simple equation:

$$x = K_A t^n$$

used by several authors (Subotic et al., 1985; Gualtieri, 2001).

Thus the purpose of our new approach is to relate directly the crystallization kinetics to both the chemical reaction order and a term depending on how much, on average, a crystal nucleus must diffuse through the solution, before colliding with another nucleus.

We considered a macroscopic system composed of two zeolitic components A and B, the second component growing at the expense of the first. We assume, according to Gualtieri (2001), that the crystal growth of the B component from the A component is not constant; it depends, in fact, on the degree of super-saturation of the solution which is influenced by the balance between dissolution of the precursor species and creation of crystal nuclei.

The idea is to study an equation which describes the decreasing rate of component A as a function of time. This rate is proportional to a power of A concentration, and the power value itself is indicative of the reaction order. Furthermore, the reaction rate depends on temperature (Arrhenius behavior) and also on the mobility of the sub components of the "global" component "A" towards reaction sites (Pasculli et al., 1999). Consequently, reaction velocity is high at first because reaction sites have been formed, but as the reaction proceeds it begins to diminish due to consumption of the A component. Let us consider a system composed of two components, A and B, the first transforming itself chemically to the second during the whole transient, thus yielding:

$$X_A(\tau) + X_B(\tau) = 1 \tag{4}$$

where $X_A(\tau)$ and $X_B(\tau)$ are the component fractions at the instant τ. At this point we assume that the decreasing rate of the first component is proportional to a power of X_A. The power exponent value is related to the chemical order of the reaction. Furthermore we observe that the decreasing rate of the first component, $dX_A/d\tau$, depends not only on a density function of the reactant's molecules but also on the mobility of the molecules through the solution.

In particular, it must depend on whether or not the molecules have enough time to reach their reaction sites. Thus, in a first approximation, the decreasing rate should be proportional, in some way, to the following ratio (Pasculli *et al.*, 1999):

$$R = \frac{\sqrt{D\tau}}{L} \qquad (5)$$

where D (in m²/s) is the diffusion coefficient of the first component through the solution, τ (in s) is the transient time already transpired, $\sqrt{D\tau}$ is the diffusion length in a simplified monodimensional geometry, and L the characteristic length of the system. We note that L depends not only on the intrinsic solution structure but also on the initial component density.

It is worthwhile pointing out that if R is zero, no reaction could take place, notwithstanding the fact that $X_A = 1$ as the transition starts. As the time increases, the rate of decrease of the first component increases to a point at which many first-component molecules have already reacted.

The simplest expression, related to the above discussion, is the following kinetic equation:

$$\frac{dX_A}{d\tau} = -K X_A^S \frac{\sqrt{D\tau}}{L} \qquad (6)$$

where: $K = K_0 e^{\frac{-\Delta G}{K_B T}}$, K_0 = kinetic constant at a fixed temperature; ΔG = free energy of a nucleus growing in the space; K_B = Boltzman constant; T = absolute temperature; and S = reaction order number.

The diffusion coefficient is a function of both the viscosity and the temperature in a more complex correlation like the Einstein or Arrhenius law.

Equation 6 is a differential equation that is easily solved by assuming a constant temperature during the whole transient. We suppose that, initially, the system is composed of only one component, thus its initial fraction is equal to unity:

$$X_{A_0} = 1$$

The solution of equation 6 is:

$$\int_{A_0(\tau)}^{A_1(\tau)} \frac{dX_A}{X_A} = \int_0^1 -K\sqrt{D}\sqrt{\tau}\, dt$$

$$X_A^{1-S} = X_{A_0}^{1-S} + k(S-1)\frac{2}{3}\sqrt{D}\tau^{3/2}$$

For $S > 1$ we obtain:

$$A = \frac{1}{\left[X_{A_0}^{1-S} + K(S-1)\frac{2}{3}\sqrt{D}\tau^{3/2}\right]^{\frac{1}{S-1}}} \qquad (7)$$

This results in a radical function and we can approximate the final part with a hyperbolic function:

$$\lim_{t \to \infty} X_A = K_0 t^{-q} \qquad (8)$$

The q term deals with the inclination of the curve describing the percentage of B, *i.e.* B reaches 100% for high q values.

From equation 8 we obtain:

$$\lim_{t \to \infty} X_A = \left[K(S-1)\frac{2}{3}\sqrt{D}\tau^{3/2}\right]^{-\left(\frac{1}{S-1}\right)} = K_0 \tau^{-q}$$

and then:

$$t^{-\left[\frac{3}{2}(S-1)\right]} = t^{-q}; \quad S = 1 + \frac{3}{2q}$$

and

$$\left[K(S-1)\frac{2}{3}\sqrt{D}\right]^{-\left(\frac{1}{S-1}\right)} = K_0$$

Thus, the equation that describes the X_B percentage at each instant is:

$$X_B = 1 - \frac{1}{\left[K(S-1)\frac{2}{3}\sqrt{D}\right]^{\frac{1}{S-1}}} \qquad (9)$$

We assume $K(S-1)\frac{2}{3}\sqrt{D} \cong 10^{-7}$ ($D = 10^{-14}$ in the case of diffusion of tritium in steel at 27°C).

In Figure 6 we report the results for fitting of the experimental data to the mathematical model. Equation 9 models the part of the run made at 80°C which is relative to complete transformation of Na-A zeolite into HS. A good fit is achieved by substituting with conditions of $S = 9/8$ and $q = 12$ in Equation 9.

CONCLUSIONS

In previous studies (Aznar and La Iglesia, 1985; Clifton, 1987; Akokelar *et al.*, 1997; Gualtieri *et al.*, 1997) zeolitic synthesis was attained by preliminary thermal activation of clay materials. In the present study, synthesis of Na-A zeolite from 10 Å halloysite is achieved without thermal pre-treatment of the raw halloysitic material. This new method of synthesis is based on a simple procedure that exploits the high intrinsic reactivity of 7 Å and 10 Å halloysite with
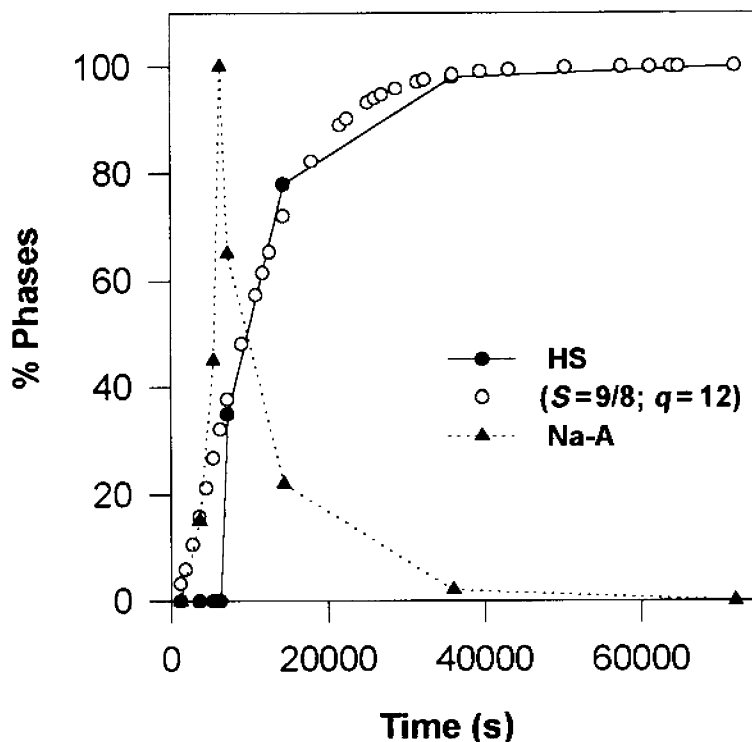
Figure 6. Plot of the degree of crystallization of Na-A and HS zeolites *vs.* time by XRD data for a synthesis run at 80°C and fitting of the experimental data with the mathematical equation 9 for $S = 9/8$ and $q = 12$.

alkalis. This method only requires the low-temperature hydrothermal treatment of 10 Å halloysite in NaOH solution.

The 10 Å halloysite is unstable in the presence of alkalis at temperatures >45°C. At temperatures below 80°C, destabilization of halloysite requires a long time and G zeolite and hydroxysodalite develop, so an isolated Na-A field does not exist. At 80°C we reach the field where only Na-A zeolite becomes stable as an isolated phase (after only 1.5 h). Achievement of a pure Na-A zeolite synthesis at such low hydrothermal temperatures and without thermal activation represents a considerable economic advantage in terms of both energy and time.

We propose a mathematical model of the crystallization kinetics to fit data for the experimental run conducted at 80°C. We consider a macroscopic system composed of two zeolitic components A and B, the second of which grows at the expense of the first. According to this model, A decreases at a rate proportional to a power of A concentration (the power value itself being indicative of the reaction order S), through a factor R (depending on the diffusion coefficient of the first component to the solution, on the transient time and on the length of the system) and a factor K (related to the free energy of a nucleus growing in the space, to the Boltzman constant, and to the temperature and the kinetic constant at a fixed temperature).

REFERENCES

Aiello, R. and Franco, E. (1968) Formazione di zeoliti per trasformazione di halloysite e montmorillonite a bassa temperatura ed in ambiente alcalino. *Rendiconti della Academia di Scienze Fisiche e Matematiche Della Società. Nazionale di Scienze Lettere ed Arti di Napoli*, **35(4)**, 165−192.

Akokelar, D., Chaffee, A. and Howe, R.F. (1997) The transformation of kaolin to low-silica X zeolite. *Zeolites*, **19**, 359−365.

Avrami, M. (1939) Kinetics of phase change. I − General Theory. *Journal of Chemical Physics*, **7**, 1103−1112.

Aznar, A.J. and La Iglesia, A. (1985) Obtención de zeolitas a

partir de arcillas aluminosas españolas. *Boletín Geológico y Minero*, **96**, 541−549.

Cardoso, A.C., Duchemin, J., Magoarou, P. and Premazzi, G. (2001) *Criteria for the identification of freshwaters subject to eutrophication. Their use for the implementation of the 'Nitrates' and Urban Waste Treatment directives.* European Commission EUR 19810, Environment and quality of life series, 90 pp.

Chapra, S.C. (1977) Total phosphorous model for the Great Lakes. *Journal of the Environmental Engineering Division, Proceedings of the American Society of Civil Engineers,* **103 (EE2),** 147−161.

Chiaudiani, G., Premazzi, G., Vismara, R., Butelli, P. and Poltronieri, P. (1988) Sostituti del fosforo nella formulazione dei detersivi. Studio di impatto ambientale. *Ingegneria Ambientale, Inquinamento e Depurazione, Quaderni,* **8**, 1−60.

Clifton, R.A. (1987) *Natural and Synthetic Zeolites.* US Bureau of Mines Information Circular 9140, 21 pp.

Costanzo, P.M. and Giese, R.F. (1985) Dehydration of synthetic hydrated kaolinites: a model for the dehydration of halloysite (10 Å). *Clays and Clay Minerals*, **33**, 415−423.

Demortier, A., Gobeltz, N., Lelieur, J.P. and Duhayon, C. (1999) Infrared evidence for the formation of an intermediate compound during the synthesis of zeolite Na-A from metakaolin. *International Journal of Inorganic Materials*, **1**, 129−134.

Di Sabatino, B., Barrese, E., Mattias, P. and Crocetti, G. (1996) L' Halloysite di Capalbio (Grosseto). Ipotesi genetica. *Mineralogica et Petrographica Acta*, **30**, 291−300.

Ehrun, M. and Advani, S.G. (1992) A B.E.M. approach to model heat flow during crystallization. *International Journal for Numerical Methods in Engineering*, **35**, 351−368.

Flaningen, E.M., Khatami, H.A. and Szymanski, H.A. (1971) Infrared structural study of zeolite frameworks. Advances in chemistry series n. 101. *Molecular Sieve Zeolites,* **16**, 201−229.

Franco, E. and Aiello, R. (1968) Trasformazioni dell'halloysite per trattamento idrotermale in ambiente alcalino. *Rendiconti della Società Italiana di Mineralogia e Petrologia*, **24(II)**, 251−269.

Gualtieri, A.F. (2001) Synthesis of sodium zeolites from a natural halloysite. *Physics and Chemistry of Minerals*, **28**, 719−728.

Gualtieri, A., Norby, P., Artioli, G. and Hanson, J. (1997) Kinetics of formation of zeolite Na-A (LTA) from natural kaolinites. *Physics and Chemistry of Minerals*, **24**, 191−199.

Kerr, P., Hamilton, P. and Pill, R. (1950) *Reference Clay Minerals*. American Petroleum Institute Project, **49**.

La Iglesia, A., Martín-Vivaldi, L. and Pozzuoli, A. (1974) Formación de zeolita A y faujasita a partir de haloisita en condiciones ambientales. *Boletín Geológico y Minero*, **85**, 442−449.

Madani, A., Aznar, A., Sanz, J. and Serratosa, J.M. (1990) ^{29}Si and ^{27}Al NMR study of zeolite formation from alkalileached kaolinites. Influence of thermal preactivation. *Journal of Physical Chemistry*, **94**, 760−765.

Pasculli, A., Baliva, A., Di Sabatino, M. and Novembre, D. (1999) Modelling of crystallization kinetic for a macroscopic two component system. Pp 233−238 in: *Proceedings of IAMG '99, Meeting of the International Association of Mathematical Geology, Trondheim, Norway* (S.J. Lippard, A. Naess and R. Sinding-Larsen, editors).

Robert, J.-L., Della Ventura, G. and Thauvin, J.L. (1989a) The infrared OH-stretching region of synthetic richterites in the system Na_2O-K_2O-CaO-MgO-SiO_2-H_2O-HF. *European Journal of Mineralogy*, **1**, 203−211.

Rocha, J. and Klinowski J. (1991) Synthesis of zeolite Na-A from metakaolinite revisited. *Journal of the Chemical Society, Faraday Transactions*, **87**, 3091−3097.

Subotic, B. Masic, N. and Smit, I. (1985) I − Analysis of particulate processes during the transformation of Zeolite A into hydroxysodalite. Pp. 207−214 in: *Zeolites* (B. Drzaj and S. Hocevar Pejovnik, editors). Elsevier, New York.

Takahashi, H. and Nishimura, Y. (1967) Formation of zeolite type A from halloysite and allophane. *Clays and Clay Minerals*, **15**, 185−186.

Takahashi, H. and Nishimura, Y. (1968) Formation of faujasite-like zeolite from halloysite. *Clays and Clay Minerals*, **16**, 399−400

Van Krevelen, D.W. (1978) Crystallinity of polymers and the means to influence the crystallization process. *Chimica*, **32**, 279−294.